

Uniaxial fatigue, creep and stress-strain responses of steel 30CrNiMo8

Josip Brnic ^{*1}, Marino Brcic ^{**1}, Sanjin Krscanski ^{1a}, Domagoj Lanc ^{1b} and Sijie Chen ^{2c}

¹ Department of Engineering Mechanics, University of Rijeka, Faculty of Engineering, Vukovarska 58, Croatia

² School of Material Science and Engineering, Henan Polytechnic University, 2001 Century Avenue, Jiaozuo 454003, P.R. China

(Received January 11, 2019, Revised March 17, 2019, Accepted March 22, 2019)

Abstract. The choice of individual material for industrial application is primarily based on knowledge of its behavior in similar applications and similar environmental conditions. Contemporary design implies knowledge of material behavior and knowledge in the area of structural analysis supported by large capacity computers. Bearing this in mind, this paper presents and analyzes the experimental results related to the mechanical properties of the material considered (30CrNiMo8/1.6580/AISI 4340) at different temperatures as well as its creep and fatigue behavior. All experimental tests were carried out as uniaxial tests. The test results related to the mechanical properties are presented in the form of engineering stress-strain diagrams. The results related to the creep behavior of the material are shown in the form of creep curves, while the fatigue of the material is shown in the form of stress – life ($S - N$) diagram. Based on these experimental results, the values of the following properties are determined: ultimate tensile strength ($\sigma_{m,20} = 696$ MPa), yield strength ($\sigma_{0.2,20} = 355.5$ MPa), modulus of elasticity ($E_{20} = 217$ GPa) and fatigue limit ($\sigma_{f,20,R=-1} = 280.4$ MPa). Results related to fatigue tests were obtained at room temperature and stress ratio $R = -1$.

Keywords: steel 30CrNiMo8; fatigue; creep; mechanical properties; Charpy impact energy

1. Introduction

In engineering practice, there are a large number of different types of structures. Under the concept of structure, as a wider term, machines are also understood. Optimal design of the structure need to be achieved taking into account available resources and limitations as well as the purpose of the structure and environmental conditions (Ohsaki 2011). The design process is an iterative process and primarily is based on high-computer capacities and a good database the material behavior. The structure is usually designed with the assumption that there is no failure in the material or the occurrence of failure during the technological process, assembling of parts, etc. However, during design and manufacturing, as well as maintenance periods of the structure, many failures can occur. Failure of the structure is usually defined as the inability of the component to function properly. In accordance with this, the causes of failures as well as failure modes (form of expression of the failures) may be divided into pre-existing ones and those that appear during service life. As the causes of failures may be mentioned (Brooks and Choudhury 2002): design errors, manufacturing defects, misuse,

structural loading, etc. Commonly observed failure modes (Collins 1993) are buckling, fatigue, creep, corrosion, yielding, etc. Based on the knowledge of causes of the failures and failure modes, the answer why and how an engineering component has failed can be obtained. The motivation of this research is to experimentally determine data on the mechanical behavior of the considered material that can serve as a reliable basis for the use of material and to avoid failures during the lifetime of the construction. Due to the possible occurrence of the mentioned failures in the construction, the paper is dealing with the experimental investigations related to creep and fatigue of the material. Conducted experimental tests related to the mechanical properties of the material as well as the investigations in the area of creep and fatigue of the material represent new material behavior data that are not available in this way in the literature. It is known that in metals, used in engineering practice, creep is considered appreciable at temperature above $0.4 T_m$, where T_m is the melting temperature of the investigated metal (Raghavan 2004). Creep is usually defined as a slow continuous deformation of considered material under constant stress (Findley *et al.* 1989). Apart from the meanings that have the mechanical properties of the material, the creep behavior and the fatigue strength of the material are of outstanding importance. Both creep and fatigue of the material belong to the commonly observed mechanical failures. Material of the structure that will operate under high temperature conditions must be creep resistant, while material that will be used in dynamic operating conditions must be resistant to fatigue and must have its fatigue limit of appropriate level. In the following part some important works by prominent authors are

*Corresponding author, D.Sc., Professor,
E-mail: brnic@riteh.hr

**Co-corresponding author, D.Sc., Professor,
E-mail: mbrbic@riteh.hr

^a D.Sc.

^b D.Sc.

^c D.Sc.

mentioned in which data are processed similar to experimentally obtained and presented data in this paper. Kluger and Lagoda (2017) have discussed the problems of allowing for mean value of torsional stress and the variability of material properties with out-of-parallel fatigue characteristics. This discussion related to several materials, including 30CrNiMo8 steel. Karolczuk and Kluger (2014) have made a comparison of the experimental and calculated fatigue lives by using criteria formulated by Findley *et al.* (1989) for several materials including 30CrNiMo8 steel. Rojas *et al.* (2018) have proposed a novel analytical model for predicting the polishing time and behavior of the surface texture removal in different metal alloys including 30CrNiMo8 steel. Bao *et al.* (2017) have investigated the variations of the residual magnetic field and its gradients on the surface of 30CrNiMo8 steel specimens with two types of defect's shape. Effertz *et al.* (2017) have described a 3D model developed in the commercial software DEFORM to study the linear friction welding process of 30CrNiMo8 high strength steel in the Hero chain. Ahangarani *et al.* (2007) have reported on a comparative study of active screen plasma nitriding and conventional dc plasma nitriding behavior of 30CrNiMo8 low-alloy steel that has been examined under various process conditions. In addition, to get an insight in the behavior of the materials with similar or different material properties and responses at prescribed environmental conditions, it is recommended to consider some other published papers. In this sense, Kaskholi and Nejad (2018) have made an analysis of time-dependent creep and life assessment of 304 L austenitic stainless steel thick pressurized truncated conical shells. Further, Brnic *et al.* (2016) have made experimental investigations and analysis of mechanical properties, creep and fatigue of 42CrMo4 steel. Arefi *et al.* (2018) have investigated history of stresses, strains, radial and circumferential displacements of a functionally graded thick-walled hollow cylinder due to creep phenomenon. In Egea *et al.* (2016), the elastoplastic effects resulting from different electropulses configurations on a wire drawing process are investigated. No data were reported in any of these published papers for the 30CrNiMo8 steel, which were considered in the manner and scope as in this work.

2. Experimental procedures: material, equipment, tests, specimens, standards

Material - under consideration was 30CrNiMo8 low alloy steel, delivered as annealed round bar of 20 mm in diameter. It contains higher carbon concentration (> 0.25%) and chromium, as well as nickel and molybdenum. This steel possesses good toughness and high strength in its heat treated conditions and at the same time retains good fatigue limit. Taking in consideration its optimum strength or toughness, it may be used in design of dynamically stressed components with large cross sections in automotive industry and generally in mechanical engineering. Finish product is usually hardened to have a high surface hardness. Chemical composition of this steel is displayed in Table 1.

The equipment- that was used in these tests refers to

Table 1 Chemical composition: 30CrNiMo8 steel

Material: 30CrNiMo8 steel (Low alloy steel)							
Designation							
Steel name (grade, quality) / i.e., letter mark of steel (EN and other norms)				Steel number (Mat. No; W. Nr; Mat. Code) / i.e., numerical designation of steel			
EN /DIN 10083-3: 2006 /17200: 30CrNiMo8 AISI 4340; BS: 823M30; AFNOR (France): 30CND8; GOST (Russia): 3KH3M3F				1.6580			
Chemical composition Mass (%)							
C	Si	Mn	P	S	Cr	Ni	Mo
0.29	0.31	0.41	0.01	0.008	2.077	1.889	0.24
Cu	Al	Sn	W	V	Co	Rest	
0.19	0.03	0.03	0.05	0.126	0.029	94.311	

tensile and impact tests. Zwick/Roell material testing machine of 400 kN capacity was used in determination of engineering stress-strain diagrams and in creep tests. Dynamic testing machine was used in fatigue tests while Charpy impact machine was used in determination of impact energy. Macroextensometer was used during testing at room temperature, while at high temperatures, high temperature extensometer was used.

Specimens – the investigated samples used in this study, differ in shape and dimensions depending on the type of test.

The test specimens used in the determination of mechanical properties and those in the creep tests were prepared (manufactured) according to the ASTM standard, ASTM: E 8M-15a. All of mentioned ASTM standards can be found in Annual Book of ASTM Standards (2015). The specimens used in fatigue tests were prepared according to ISO 12107 (2012) standard.

Standards – according to which the tests were performed, are as follows. Tensile tests leading to engineering stress- strain diagrams at room temperature were carried out according to ASTM: E 8M-15a standard. Tensile tests that relate to high temperatures were carried out according to ASTM: E21-09 standard, while those tests that relate to creep testing were carried out according to ASTM: E 139-11 standard. Fatigue tensile tests were carried out in accordance with above-mentioned ISO 12107 (2012) standard.

3. Experimental results and discussion

3.1 Mechanical properties versus temperature

Based on the obtained engineering stress-strain diagrams at different temperatures, it is possible to determine mechanical properties and their temperature dependence. It is visible that ultimate tensile strength and yield strength of this steel at room temperature are quite

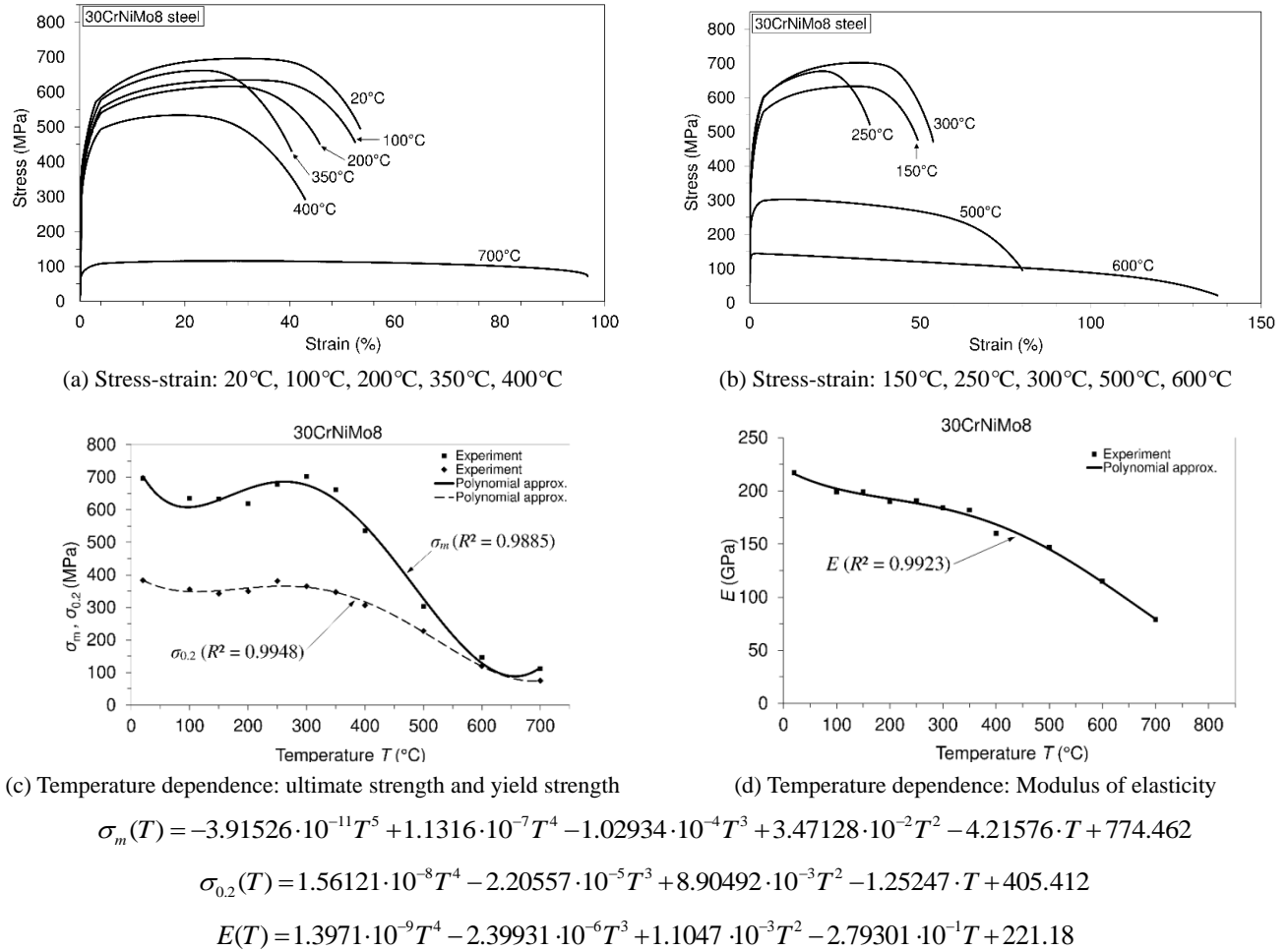


Fig. 1 Engineering stress-strain diagrams and temperature dependence of mechanical properties

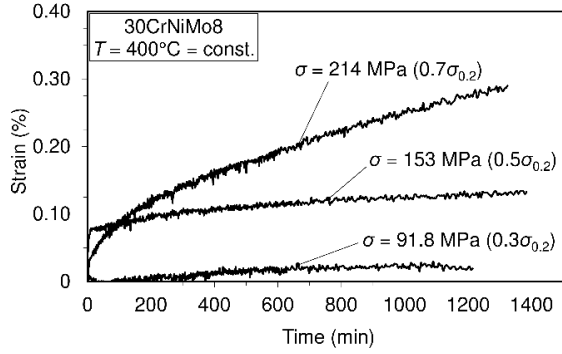
high (696 MPa / 383 MPa). After the room temperature both of mentioned properties decrease until the temperature of 100°C and after that point they again increase reaching their maximum at 300°C (702 MPa / 365 MPa). Test results relative to mechanical properties justify the use of this material in design of highly stressed engineering components. Engineering stress-strain diagrams and temperature dependences of the mechanical properties are shown in Fig. 1.

The mechanical properties of materials that define the behavior of materials under certain conditions are of paramount importance for the design process of engineering elements. They represent the most reliable data for evaluating the behavior of elements under the prescribed conditions of exploitation. As it is visible from Figs. 1(a)-(b), experimentally obtained data of considered properties, are shown as discrete points while interpolated curves (polynomials) represent continuous change of the considered values (properties). These curves represent simulated / modeled curves that, with specific accuracy, replace actual data (experimentally obtained data). A coefficient called coefficient of determination (R^2) is established as a measure of accordance of simulated and real (measured) values. It gives information about how fit a model is Draper and Smith (1998).

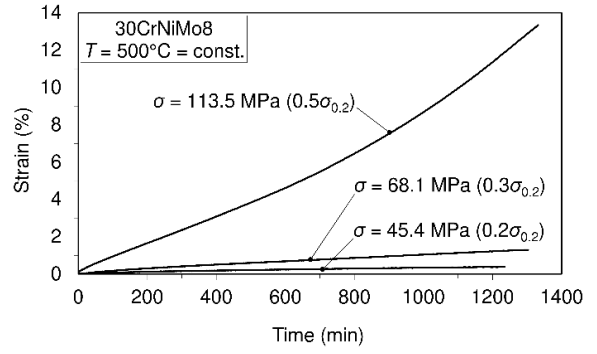
3.2 Creep testing and modelling

During these investigations, short-term creep tests were performed. These tests are suitable for determining the resistance of the material to creep in the cases of its exposure to a short-term increase in temperature, such as an example of fire, sudden heating of the element, etc. In any case, knowledge of strains during creep is of paramount importance because exceeding the prescribed level of deformation can result in the element being no longer in function for which it was designed. In Fig. 2 some of short-time creep tests are shown. It is well known that experiments in engineering practice provide the most relevant data but at the same time they can be very expensive and can consume a lot of time. From the other hand, creep process can be simulated / modeled / predicted. Generally, creep behavior can be modeled using formulas or rheological models. Further, modeling can be performed in such a way that creep strain is monitored during the time while stress and temperature are kept constant, or only temperature is kept constant, or none parameter is kept constant. The last mentioned case is the most general case and it is performed in this investigation using formula (Brnic *et al.* 2014)

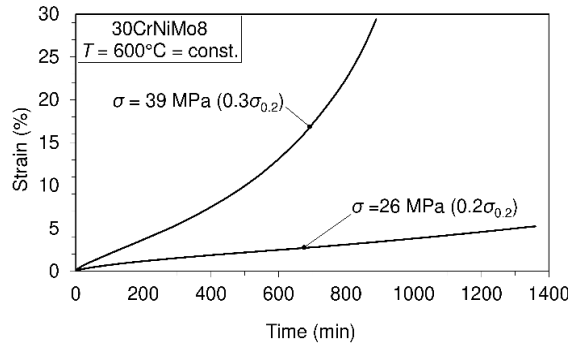
$$\varepsilon(t) = D^{-T} \sigma^p t^r \quad (1)$$



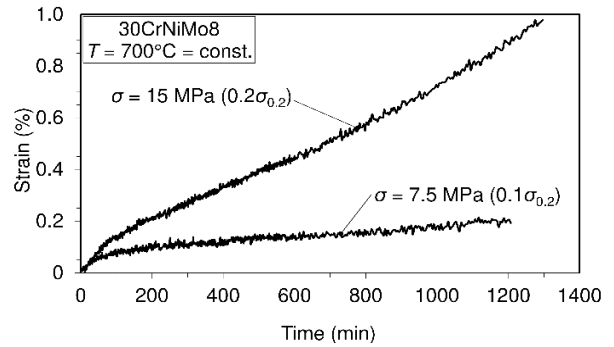
(a) Creep test at temperature of 400°C



(b) Creep test at temperature of 500°C

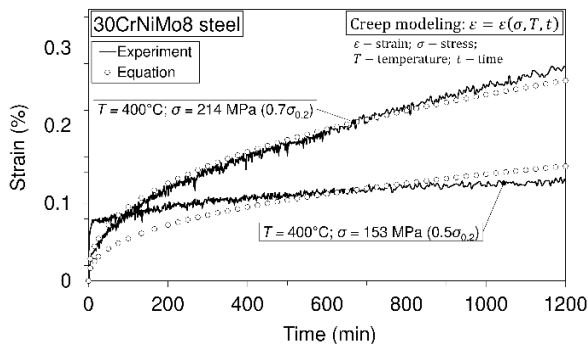


(c) Creep test at temperature of 600°C

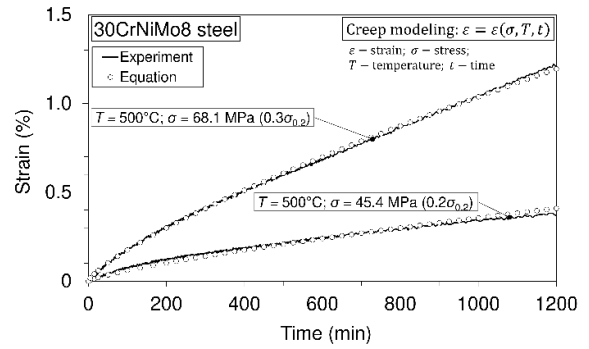


(d) Creep test at temperature of 700°C

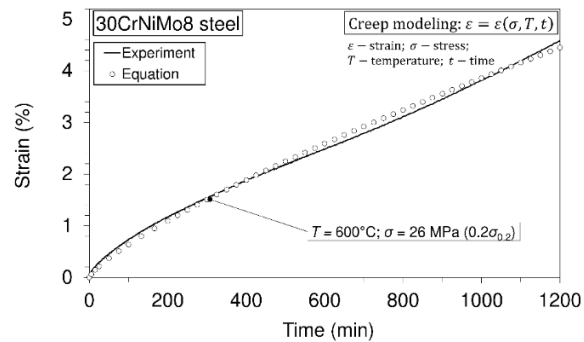
Fig. 2 Short-time creep tests: 30CrNiMo8 steel



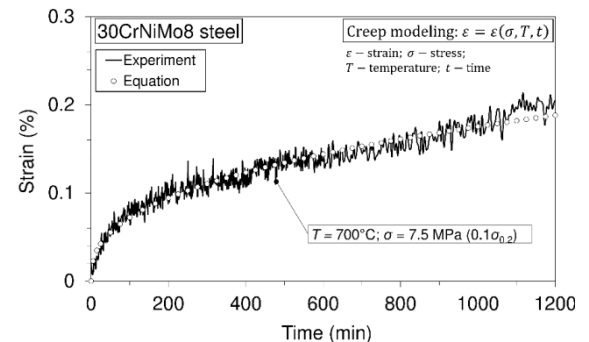
(a) Creep modeled curves at temperature of 400°C



(b) Creep modeled curves at temperature of 500°C



(c) Creep modeled curve at temperature of 600°C



(d) Creep modeled curve at temperature of 700°C

Fig. 3 Creep modeled tests: 30CrNiMo8 steel

Table 2 Creep modeling data

Material: 30CrNiMo8 (1.6580)						
Creep strain - time dependence model:	Equation * $\varepsilon(t) = D^{-T} \sigma^p t^r$					
For all used models and considered creep processes is valid:	$\varepsilon(t) = \varepsilon(\sigma, T, t)$; Time (min) = 1200					
Creep processes (tests) were carried out at temperatures and stresses listed below						
Constant temperature ($T^\circ\text{C}$)	400	500	600	600	700	700
Applied constant stress level σ (MPa)	153	214	45.4	68.1	26	7.5
$\sigma = x \cdot \sigma_{0.2}$	$x = 0.5$	$x = 0.7$	$x = 0.2$	$x = 0.3$	$x = 0.2$	$x = 0.1$
Parameters	Parameters (D, p, r) valid for:					
	$x = 0.5 - 0.7$	$x = 0.2 - 0.3$	$x = 0.2$	$x = 0.1$		
D, p, r In accordance with above given equation*	$D(T) = 1.5402615 \cdot 10^{-7} T^3 - 2.3396989 \cdot 10^{-4} T^2 +$ $+ 1.1679209 \cdot 10^{-1} T - 18.045188$					
	$p(T) = 4.6290869 \cdot 10^{-6} T^3 - 7.0168444 \cdot 10^{-3} T^2 +$ $+ 3.501245 T - 572.40703$					
	$r(T) = -6.843823 \cdot 10^{-9} T^3 - 7.9323219 \cdot 10^{-6} T^2 +$ $+ 1.503727 \cdot 10^{-2} T - 3.9069747$					

In Eq. (1) there are: σ - stress, T - temperature, t - time and D , p and r are parameters.

Modeled creep curves according to Eq. (1) are shown in Fig. 3, while data related to creep modeling are given in Table 2.

By analyzing the results of the short-term creep of this steel, it can be said, that it can be considered resistant to creep at a temperature of 400°C regardless of the applied stress level. Considering the creep process at a temperature of 500°C , it is visible that this steel is resistant to creep if the applied stress level does not exceed 20% of the yield strength at this temperature. As for the temperature of 600°C – 700°C , this material is creep resistant but at very low applied stress. As is apparent, with regard to simulation / modeling of the creep process, the formula used can well simulate the creep process practically in all considered cases related to the first and second creep stages.

3.3 Fracture toughness assessment based on Charpy impact energy

Two of material properties are usually mentioned as the most important ones in engineering design. One of them is yield strength which is considered the design criterion in the design of the structure against the plastic deformation. Another one is fracture toughness that is a criterion for design structure against fracture (Blinn and Williams 1997). Fracture toughness that is critical value of stress intensity factor, and is usually designated as K_{Ic} , is determined experimentally. Since the manufacture of the specimens regarding their sizes and technology of the manufacture is quite demanding, exist other methods to determine approximate values of the fracture toughness. One of the recognizable intermediary methods is Charpy impact method that is also experimental method. It should be said that although it is an experimental method it is a laboratory test since a material is not taken from a real structure. However, there are some correlations between Charpy

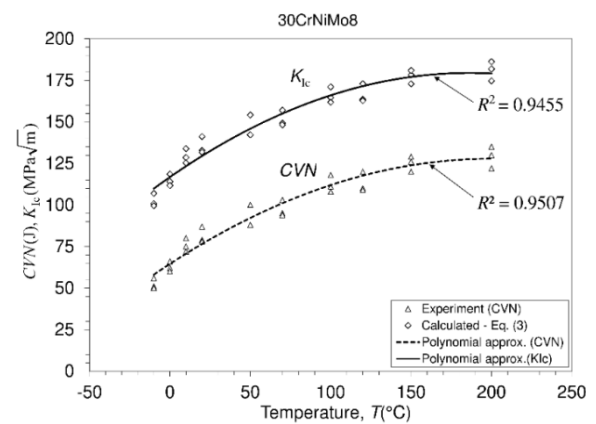
impact energy (CVN) obtained by Charpy machine and fracture toughness. As a well known formula that relates CVN energy and fracture toughness is Roberts-Newton formula (Chao *et al.* 2007)

$$K_{Ic} = 8.47(CVN)^{0.63} \quad (2)$$

In Eq. (2), CVN means Charpy V- notch impact energy measured in Joules. The calculated value of fracture toughness using Eq. (2) is temperature independent. Measured values of Charpy impact energy as well as calculated values of fracture toughness are displayed in Fig. 4.

3.4 Uniaxial fatigue testing and fatigue limit

Fatigue is, as previously said, one of commonly observed failure mode in engineering practice and it is of



$$CVN(T) = -1.57651 \cdot 10^{-3} T^2 + 6.31758 \cdot 10^{-1} T + 64.5729$$

$$K_{Ic}(T) = -1.80278 \cdot 10^{-3} T^2 + 6.72279 \cdot 10^{-1} T + 116.776$$

Fig. 4 Charpy impact energy and fracture toughness

importance for components subjected to repeated loads. Fracture can be considered as a result of the fatigue of material. In this study investigation of the fatigue was performed on unnotched specimens subjected to uniaxial stress at stress ratio of $R = -1$ at room temperature. Each industrial design seeks to be implemented in such a way that the final design is optimal. In the design process, thenumerical analysis of the behavior of the construction is based on an experimental analysis of the behavior of material in similar conditions of exploitation. In this sense, for the construction in its entirety, or for any engineering element, it is of importance to know how behaves the material, which is subjected to repeated load. Experimental analyzes show that static strength of the material under repeated load can be significantly reduced. This is the reason that dynamically stressed components need to be designed in accordance with the so-called fatigue limit. Although optimal design implies the best design, there are a large number of possible failures which can reduce the quality as well as the safety of the product. This means that fatigue criteria that include fatigue life models related to the durability of service life must be taken into account. Fatigue tests were performed to obtain fatigue strength data at the considered number of cycles as well as fatigue limit data. Of course, selected material for testing, stress ratio as well as adopted data related to number of cycles to failure, depend on the purpose of the designed structure and its working life conditions. In this investigation the so-called stress-life (stress versus the number of cycles to failure) was used. In the fatigue testing procedures, for each applied stress level, several specimens were tested to their failures (fractures), and in coordinate system these points were recorded. Namely, each fatigue test in the stress-life coordinate system generates one point. During testing procedures some of specimens can failed while some of them remain unbroken. For steel alloys the number of the cycles to failure in infinite fatigue life (infinite fatigue region) is usually adopted as 10 million cycles. When reached points based on failed specimens are approximated / modeled by logarithmic line then so-called inclined line is obtained and it represents fatigue finite life region. From the other hand, data recorded in infinite fatigue region that originates from unbroken specimens, when modeled as

Table 3 Data related to failed (♦) and non-failed (○) specimens used in modified staircase method

Stress ratio $R = -1$, room temperature							
Stress σ_i /MPa	Specimen						
	1	2	3	4	5	6	7
290			♦		♦		♦
285		○		♦		♦	
280	○						

Table 4 Data analysis for modified staircase method

Stress ratio $R = -1$, room temperature, f -failed				
Stress σ_i /MPa	Stress level, i	f_i	if_i	i^2f_i
290	2	3	6	12
285	1	2	2	2
280	0	0	0	0
$\sum f_i, if_i, i^2f_i$		5	8	14

Table 5 Constants (A, B, C and D) according to ISO 12107

Stress ratio $R = -1$	
Formula	30CrNiMo8
$A = \sum i \cdot f_i$	8
$B = \sum i^2 \cdot f_i$	14
$C = \sum f_i$	5
$D = \frac{B \cdot C - A^2}{C^2}$	0.24

straight-line forms finite fatigue region and in accordance to the appropriate standard (earlier mentioned ISO standard), someone can calculate fatigue limit. However, fatigue as a failure that occurs due to repetitive load can cause fracture that can occur at a stress level that is much lower than fracture stress corresponding to a monotonic tensile load. In Fig. 5 is presented stress versus cycles to failure diagram for investigated material 30CrNiMo8. Fatigue tests were performed at room temperature and at stress ratio of $R = -1$. Fatigue limit (endurance limit) was calculated using modified staircase method. Two regions, and that, infinite fatigue region and finite fatigue region are approximated (modeled) by two straight lines. In diagram, failed specimens during testing are marked as (♦) points while those that remained unbroken are marked as (○) points. In addition, procedure for determine fatigue limit using modified staircase method can be given as follows. First, in Table 3, and based on the fatigue diagram, are shown data for staircase method related to failed (♦) and non-failed (○) specimens. In addition, in Table 4 the mentioned data are analyzed, while determination of constants A, B, C and D is presented in Table 5.

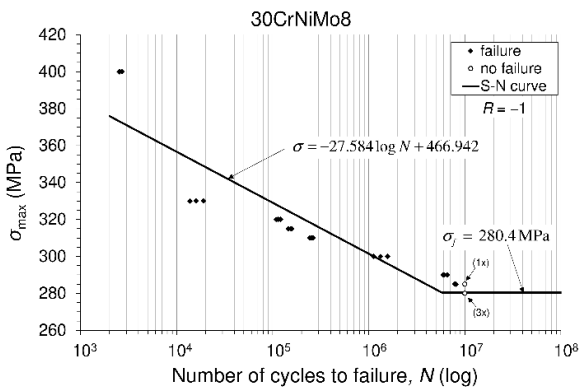


Fig. 5 Fatigue tests: experimental and approximated S-N curve, $R = -1$, room temperature

Since within this paragraph the term fatigue limit (endurance limit) was discussed (Dowling 2013, Suresh 2003 and Brnic 2018), it is necessary to explain its meaning. When during the fatigue testing at the prescribed conditions (stress ratio, temperature, etc.) and regardless of the number of the cycles (sometimes prescribed, let say 10 mil.) the specimen remains unbroken, fatigue limit (endurance limit) has been reached, which is the strength that corresponds to the stress associated with this prescribed number of the cycles. This means that there is a theoretical stress level for prescribed stress ratio and number of cycles below which the material will not fail. Finally, when in accordance with ISO standard (ISO 12107, 2012) the data analysis is done and the constants are calculated, further procedure related to fatigue limit determination is defined as

$$\sigma_{f(P,1-\alpha)} = \bar{\mu}_y - k_{(P,1-\alpha,\nu)} \cdot \bar{\sigma}_y, \quad (3)$$

where:

- $\bar{\mu}_y$, the mean fatigue strength, that is defined as

$$\bar{\mu}_y = \sigma_0 + d \left(\frac{A}{C} - \frac{1}{2} \right) \quad (4)$$

and “d” is the stress step, → Table 4,

- $k_{(P,1-\alpha,\nu)}$, the coefficient for the one sided tolerance limit for a normal distribution,
- $\bar{\sigma}_y$, the estimated standard deviation of the fatigue strength that is calculated as

$$\bar{\sigma}_y = 1.62 \cdot d(D + 0.029). \quad (5)$$

In accordance with the used standard, the value $\nu = n - 1 = 6$, where n is the number of items in a considered group. For a desired probability of $P = 10\%$ and taking a confidence level $(1 - \alpha) = 90\%$, in accordance with the table B1 (ISO 12107 2012), it is: $k_{(P,1-\alpha,\nu)} = k_{(0.1;0.9;6)} = 2.333$ In accordance with Eq. (4), it is

$$\begin{aligned} R = -1 &\rightarrow \bar{\mu}_y = \sigma_0 + d \left(\frac{A}{C} - \frac{1}{2} \right) \\ &= 280 + 5 \left(\frac{8}{5} - \frac{1}{2} \right) = 285.5 \text{ Mpa.} \end{aligned}$$

Similar value can be obtained based on Table 4

$$\begin{aligned} R = -1 &\rightarrow \bar{\mu}_y \\ &= \frac{280 + 285 + 290 + 285 + 290 + 285 + 290}{7} \\ &= 286.4 \text{ MPa.} \end{aligned}$$

The estimated standard deviation of the fatigue, Eq. (5), is

$$\begin{aligned} R = -1 &\rightarrow \bar{\sigma}_y = 1.62 \cdot d(D + 0.029) \\ &= 1.62 \cdot 5(0.24 + 0.029) = 2.179 \text{ MPa.} \end{aligned}$$

Fatigue limit in accordance with Eq. (3), is

$$\begin{aligned} R = -1 &\rightarrow \sigma_{f(0.1;0.9;6)} = \bar{\mu}_y - k_{(P,1-\alpha,\nu)} \cdot \bar{\sigma}_y \\ &= 285.5 - 2.333 \cdot 2.179 = 280.4 \text{ MPa.} \end{aligned}$$

Calculated value of the fatigue limit, based on the fatigue testing at stress ratio of $R = -1$, indicates that its value is 40.2% ($= 280.4/696$) compared to the ultimate monotonic stress.

3.5 Analysis of the microstructure of the material used in the tests

In this study a basic microstructure analysis was performed which refers to the as-received material (first specimen), the material subjected to creep (second specimen), and the one under fatigue (third specimen). As-received material was annealed material. The material subjected to creep refers to creep process that is performed at 500°C at the stress level of 113.5 MPa, while the material subjected to fatigue refers to the fractured specimen. Each of the specimens for the three mentioned cases had a diameter of 20 mm. For microstructure analysis of as-received material as well as of material previously subjected to creep an optical microscope was used, while SEM (scanning electron microscope) was used in analysis of the material that has been subjected to fatigue. The last mentioned microscope is such type of electron microscope producing images of a sample by scanning the surface with a focused beam of electrons. In Fig. 5 are shown optical micrographs that are related to as-received material and material that is previously subjected to creep. Based on microstructure analysis of the material structure of as-received material, Fig. 6(a), it is visible that the matrix

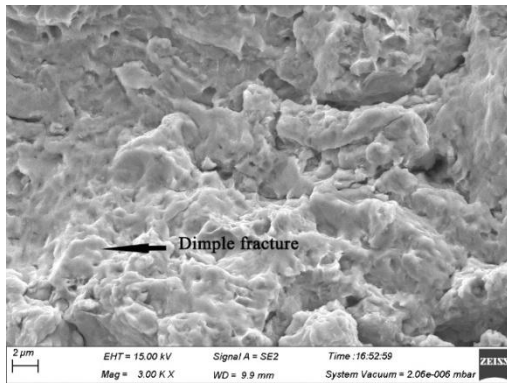


(a) As-received material

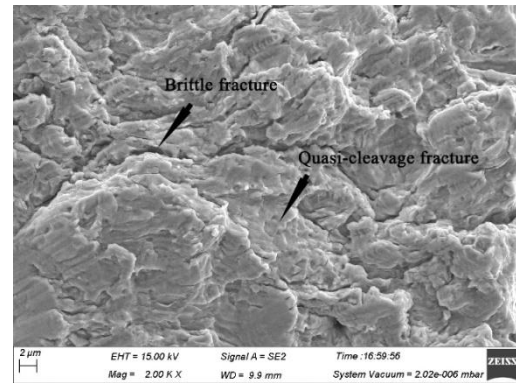


(b) After the creep process performed at: 500°C/113.5 MPa/1200 min

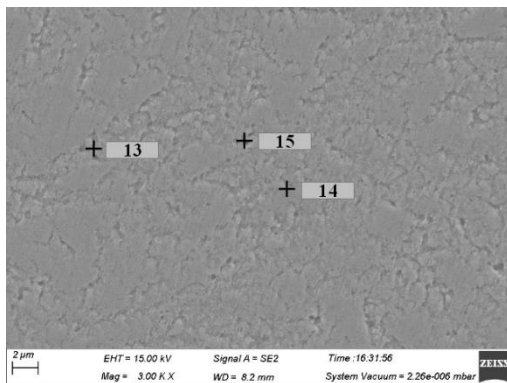
Fig. 6 Optical micrographs: steel 30CrNiMo8, 3% nitric acid, cross-section of the specimen, 1000x



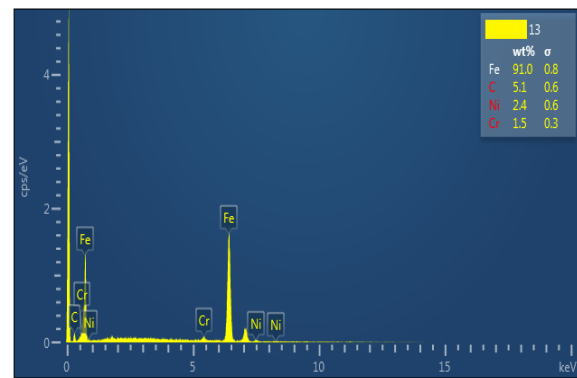
(a) Dimple fracture (performance of ductile fracture), 3000x



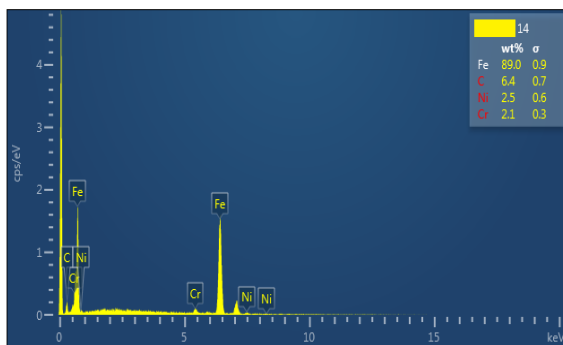
(b) Cracks – cleavage planes (brittle fracture), 2000x



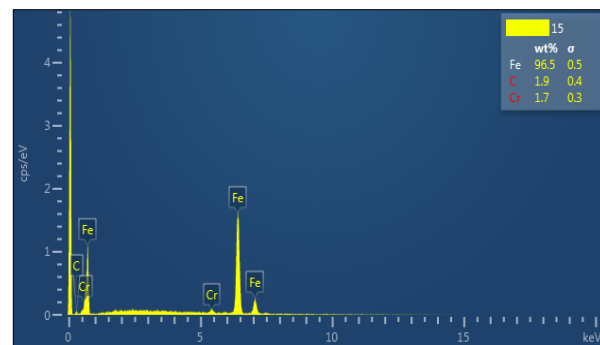
(c) SEM micrograph-cross-section of the specimen, 3000x



(d) Composition - position 13 on the SEM micrograph



(e) Composition - position 14 on the SEM micrograph



(f) Composition - position 15 on the SEM micrograph

Fig. 7 SEM of fractured specimen subjected to uniaxial fatigue (± 300 MPa, 1.567.444 cycles)

consists of evenly distributed pearlite and ferrite and carbide precipitation at the grain boundaries. Regarding the analysis related to material previously subjected to creep, Fig. 6(b), the result shows that the content of alloy elements in ferrite decreases while the contents of alloy elements in carbide increases, and that carbides increasingly coupled during creep. As said above, images obtained by scanning electron microscope can be used to analyze the fracture surface of the specimen that has been subjected to fatigue; Fig. 7. It is visible that many dimples exist which are the performance of ductile fracture, and they are of the size of about $0.5 \mu\text{m}$, Fig. 7(a). It is also evident that there are many cracks along the lines of which many cleavage planes exist characterizing brittle fracture, Fig. 7(b). It is therefore a mixed fracture mechanism.

In Fig. 7(c) SEM micrograph of cross-section of fractured specimen is presented. It can be seen that at the grain boundaries are mainly Fe-C intermetallic compounds containing a small amount of Ni and Cr compounds. The existence of these compounds makes the material more strength while the toughness decreases. The details (d, e, f) in Fig. 7 illustrate the composition of the material at the indicated points.

4. Conclusions

The data obtained by this research is of utmost concern to the the designers of the structures that will be produced from 30CrNiMo8 steel. The experimental results of the

research refer to mechanical properties of the material at different temperatures, the behavior of the material under creep as well as the fatigue of the material undergoing a fully reversed loading tests (symmetrical / alternate cycle, $R = -1$). All experimental tests were performed as uniaxial stress tests. Results that refer to mechanical properties are displayed in the form of engineering stress-strain diagrams, those that relate to material creep behavior in the form of creep curves, while those that refer to fatigue are presented in the form of $S-N$ diagram. Mechanical properties characterized by numerical values are as follows: ultimate tensile strength at room temperature and temperature of 700°C ($\sigma_{m,20} = 696 \text{ MPa}$, $\sigma_{m,700} = 116 \text{ MPa}$); yield strength at the same considered temperatures ($\sigma_{0,2,20} = 355.5 \text{ MPa}$, $\sigma_{0,2,700} = 75 \text{ MPa}$). As for the resistance to creep, it can be said that this material can be treated as creep resistant to short-time creep at 400°C . At the temperature of 500°C this material is creep resistant if applied stress does not exceed 50% of yield stress at this temperature. As the result of this investigation, using the proposed formula, creep modeling of some creep tests is also presented. Behavior on the fatigue of this material shown by $S-N$ curve has two regions, and that, finite fatigue region displayed by inclined line and infinite fatigue region represented by horizontal line. Endurance limit (fatigue limit) was determined by modified staircase method and it amounts (at room temperature): $\sigma_{f,20,R=-1} = 280.4 \text{ MPa}$.

Acknowledgments

This work has been financially supported by the University of Rijeka within the projects: uniri-technic-18-42, "Investigation, analysis and modeling the behavior of structural elements stressed at room and high temperatures" and uniri-technic-18-200, "Failure analysis of materials in marine environment".

References

- Ahangarani, Sh., Sabour, A.R. and Mahboubi, F. (2007), "Surface modification of 30CrNiMo8 low-alloy steel by active screen setup and conventional plasma nitriding methods", *Appl. Surf. Sci.*, **254**(5), 1427-1435.
- Annual Book of ASTM Standards (2015), Metals - Mechanical Testing; Elevated and Low-Temperature Tests; Metallography, Vol. 03.01, ASTM International, Baltimore, MD, USA.
- Arefi, M., Nasr, M. and Loghman, A. (2018), "Creep analysis of the FG cylinders: time-dependent non-axisymmetric behavior", *Steel Compos. Struct., Int. J.*, **28**(3), 331-347.
- Bao, S., Fu, M., Lou, H. and Bai, S. (2017), "Defect identification in ferromagnetic steel based on residual magnetic field measurements", *J. Magnet. Magnet. Mater.*, **441**, 590-597.
- Blinn, M.P. and Williams, R.A. (1997), Design for fracture toughness, ASTM Handbook, Vol. 20, Materials Selection and Design, Dieter, G.E., Volume Chair, ASM International, USA, pp. 533-544.
- Brcic, J. (2018), *Analysis of Engineering Structures and Material Behavior*, John Wiley & Sons, Chichester, UK.
- Brcic, J., Turkalj, G., Krscanski, S., Lanc, D., Canadija, M. and Brcic, M. (2014), "Information relevant for the design of structure: ferritic-heat resistant high chromium steel X10CrAlSi25", *Mater. Des.*, **63**, 508-518.
- Brcic, J., Canadija, M., Turkalj, G., Krscanski, S., Lanc, D., Brcic, M. and Zeng, G. (2016), "Short-time creep, fatigue and mechanical properties of 42CrMo4 - Low alloy structural steel", *Steel Compos. Struct., Int. J.*, **22**(4), 875-888.
- Brooks, C.R. and Choudhury, A. (2002), *Failure Analysis of Engineering Materials*, McGraw-Hill, New York, NY, USA.
- Chao, Y.J., Ward, J.D. and Sands, R.G. (2007), "Charpy impact energy, fracture toughness and ductile-brittle transition temperature of dual-phase 590 Steel", *Mater. Des.*, **28**, 551-557.
- Collins, J.A. (1993), *Failure of Materials in Mechanical Design*, John Wiley & Sons, New York, NY, USA.
- Dowling, N.E. (2013), *Mechanical Behavior of Material*, (4th ed.), Pearson, New York, NY, USA.
- Draper, N.R. and Smith, H. (1998), *Applied Regression Analysis*, Wiley - Interscience Publications, USA.
- Effertz, P.S., Fuchs, F. and Enzinger, N. (2017), "3D modelling of flash formation in linear friction welded 30CrNiMo8 steel chain", *Metals*, **7**(10), 449. DOI: 10.3390/met7100449
- Egea, A.J.S., Rojas, H.A.G. and Celetano, D.J. (2016), "Mechanical and metallurgical changes on 308L wires drawn by electropulses", *Mater. Des.*, **90**, 1159-1169.
- Findley, W.N., Lai, J.S. and Onaran, K. (1989), *Creep and Relaxation of Linear Viscoelastic Materials*, Dover Publications, New York, NY, USA.
- ISO 12107:2012 (E) (2012), Metallic materials — Fatigue testing — Statistical planning and analysis of data.
- Karolczuk, A. and Kluger, K. (2014), "Analysis of the coefficient of normal stress effect in chosen multiaxial fatigue criteria", *Theor. Appl. Fract. Mech.*, **73**, 39-47.
- Kaskholi, M.D. and Nejad, M.Z. (2018), "Time-dependent creep analysis and life assessment of 304 L austenitic stainless steel thick pressurized truncated conical shells", *Steel Compos. Struct., Int. J.*, **28**(3), 349-362.
- Kluger, K. and Lagoda, T. (2017), "A new algorithm for estimating fatigue life under mean value of stress", *Fatigue Fract. Eng. Mater. Struct.*, **40**(3), 448-459.
- Ohsaki, M. (2011), *Optimization of Finite Dimensional Structures*, CRC Press, New York, NY, USA.
- Raghavan, V. (2004), *Materials Science and Engineering*, Prentice-Hall of India, New Delhi, India.
- Rojas, G.H.A., Egea, S.A.J., Rodríguez, T.J.A., Fuentes, L.J. and Peiró, J.J. (2018), "Estimation of the polishing time for different metallic alloys in surface texture removal", *Mach. Sci. Technol.*, **22**(4), 729-741.
- Suresh, S. (2003), *Fatigue of Materials*, (2nd ed.), Cambridge University Press, Cambridge, UK.

CC